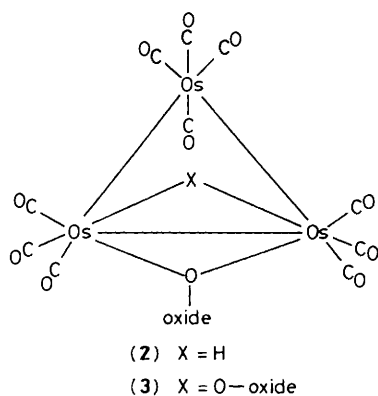


Spectroscopic Studies on Adsorbed Metal Carbonyls. Part 3.† Interaction of $[\text{Os}_3(\text{CO})_{12}]$ with Silica, Alumina, and Titania‡

Stephen L. Cook, John Evans,* and Gregory S. McNulty
 Department of Chemistry, The University, Southampton SO9 5NH
 G. Neville Greaves
 S.E.R.C. Daresbury Laboratory, Daresbury, Warrington WA4 4AD

The interaction of $[\text{Os}_3(\text{CO})_{12}]$ on silica, alumina, and titania gives, as the initially observed adsorbate, $[\text{Os}_3\text{H}(\text{CO})_{10}(\mu\text{-O-oxide})]$ (2) (on silica) or $[\text{Os}_3(\text{CO})_{10}(\mu\text{-O-oxide})(\text{OH})]$ (3). Following analyses of the model compounds $[\text{Os}_3\text{XY}(\text{CO})_{10}]$ ($\text{X} = \text{Y} = \text{H}$; $\text{X} = \text{H}$, $\text{Y} = \text{OMe}$; $\text{X} = \text{Y} = \text{OEt}$), the structure of this species on alumina was investigated by Os *L* (III) edge extended *X*-ray absorption fine structure. Both (2) and (3) can be fitted to the data, but the latter affords more reasonable Debye–Waller factors. Subsequent pyrolysis generates a mixture of $[\text{Os}(\text{CO})_3]_n$ and $[\text{Os}(\text{CO})_2]_n$ species. This process is reversible on silica. Attempts to simulate the $\nu(\text{CO})$ absorptions of a ^{13}C O-enriched version of the pyrolysis products to simple mono- and di-nuclear models were unsuccessful. This evidence, together with the electronic absorption spectra of these materials, suggests a trimeric array as the smallest likely unit, probably with some metal–metal bonding. A by-product from the reaction with alumina and titania was $[\text{Os}_3\text{H}(\text{Cl})(\text{CO})_{10}]$. Interaction of $[\text{Os}_3(\text{CO})_{12}]$ with a hydroxylated cleaved mica crystal in refluxing *n*-octane gave rise to the pyrolysis products $[\text{Os}(\text{CO})_3]_n$ and $[\text{Os}(\text{CO})_2]_n$.

In this Series we have investigated the adsorption of metal carbonyl clusters on the common high surface area oxide supports by detailed studies of the $\nu(\text{CO})$ i.r. absorptions of the surface species in conjunction with electronic spectroscopy.^{1,2} We now present similar studies applied to the chemistry of $[\text{Os}_3(\text{CO})_{12}]$ (1) on these supports including some extended *X*-ray absorption fine structure (EXAFS) results. The first identifiable stage of chemisorption on silica has been shown to give rise to $[\text{Os}_3\text{H}(\text{CO})_{10}(\mu\text{-O-oxide})]$ (2). The same type of surface species has also been proposed for Al_2O_3 ,^{3–6} TiO_2 ,⁵ ZnO ,⁵ and MgO ⁷ environments. However, differentiation from an alternative, $[\text{Os}_3(\text{CO})_{10}(\mu\text{-O-oxide})_2]$ (3), is difficult by



most spectroscopic techniques. Fits of the EXAFS experimental data to both structural types were possible on alumina, with the latter requiring more realistic Debye–Waller factors for the Os–O shell;⁸ we now present a full report of this work. Subsequent reactions of the adsorbed carbonyl give rise to species which exhibit relatively simple but broad $\nu(\text{CO})$ i.r.

spectra. The Os:CO ratio of these species is oxide dependent,⁹ varying between 1:2 and 1:3. Evidence has been obtained on silica which indicates $\text{Os}(\text{CO})_2$ and $\text{Os}(\text{CO})_3$ units coexist and are in equilibrium.⁴ Structural proposals for these species are contradictory. Most reports, considering the apparent simplicity of the $\nu(\text{CO})$ i.r. bands, favour mononuclear sites,^{7,10} or dimeric and polymeric units without metal–metal bonds.^{4,5} The geometry of these as vibrationally isolated units has been estimated from the relative intensities of the $\nu(\text{CO})$ i.r. absorptions.¹¹ An e.s.r. study of these species on alumina revealed three paramagnetic sites under various conditions, but in all cases the majority of the osmium was e.s.r. silent.¹² However, evidence, including electron microscopy, has suggested a larger aggregate of metal atoms, perhaps three¹³ or 12 metal atoms.⁹

In view of their catalytic activity,^{4–7,9,10} these materials are of some interest. If the pyrolysed samples do indeed contain mononuclear sites, then this should be readily confirmed by ^{13}C O isotopic substitution experiments and computer simulations of the i.r. spectra of the resulting materials.

Experimental

The general preparative procedures, vibrational and electronic spectroscopic measurements, and computation were carried out as previously described.^{1,2} $[\text{Os}_3(\text{CO})_{12}]$ was prepared according to ref. 14 and enriched with ^{13}C O in mesitylene solution under ^{13}C O at 160 °C for 3 d in a sealed vessel. The ^{13}C O content was determined as being in the range 70–80% by matching the experimentally observed mass spectral isotope pattern with calculated values.

Interaction of $[\text{Os}_3(\text{CO})_{12}]$ (1) with Oxides.—These reactions were carried out as in ref. 2. A suspension of the oxide was refluxed in a solution of (1) in a hydrocarbon solvent. The oxides used were Aerosil 200, Aluminoxid C, and Titanoxid P25 supplied by Degussa, and the solvents used were cyclohexane, *n*-octane and nonane (silica), cyclohexane, *n*-heptane and *n*-octane (alumina), and *n*-heptane (titania).

† Part 2 is ref. 2.

‡ Non-S.I. units employed: Torr = (101 325/760) N m⁻²; dyn = 10⁻⁵ N.

Disc Pyrolysis Experiments.—Samples of species (A) and (C), produced by the solution reactions of $[\text{Os}_3(\text{CO})_{12}]$ (1) with the appropriate oxide, were pressed into thin 14-mm diameter discs which were pyrolysed *in vacuo* (0.1 Torr). If required, CO was admitted to the cell and the system isolated whilst the disc was heated for the required time. The system was then evacuated before i.r. spectra were recorded.

Powder Pyrolysis Experiments.—Some of the disc experiments were paralleled by pyrolysis and exposure to CO in a resealable vessel on a powdered sample.

Attenuated Total Internal Reflectance (ATR) Experiment.—A sample of muscovite mica (14 mm × 5 mm) was cleaved and hydroxylated in refluxing water for 2 d. The sample was dried *in vacuo*, and then transferred to a refluxing n-octane solution of $[\text{Os}_3(\text{CO})_{12}]$ (1). After 15 h, the mica was washed and dried *in vacuo*. I.r. spectra were recorded on a Wilks model 45A microsampling apparatus using a 25-reflection KRS-5 internal reflectance element.

EXAFS Measurements and Analysis.—The Os L(III) edge X-ray absorption spectra were recorded on the synchrotron radiation source (SRS) at the S.E.R.C. Daresbury Laboratory in the transmission mode. The model compounds $[\text{Os}_3(\text{CO})_{12}]$, $[\text{Os}_3(\mu\text{-H})_2(\text{CO})_{10}]$, $[\text{Os}_3(\mu\text{-H})(\text{CO})_{10}(\mu\text{-OMe})]$, and $[\text{Os}_3(\text{CO})_{10}(\mu\text{-OEt})_2]$ were obtained on Station 7.4 using a Si(220) channel cut monochromator. A similar procedure was employed for the data on the initial $[\text{Os}_3(\text{CO})_{12}]$ -alumina product, (C), with four spectra being averaged. The spectrum of species (D) on alumina was obtained with a single scan on Station 7.1 using a Si(111) order sorting monochromator.

Calibration and background subtraction were performed using the programs EXCALIB and EXBACK respectively, in the SRS Program Library.¹⁵ Analysis of the EXAFS data was carried out by curved wave procedures¹⁶ within the program EXCURVE¹⁷ on the NAS AS-7000 computer at the Daresbury Laboratory. *Ab initio* phase shifts were employed from the EXAFS Data Base¹⁸ with the absorbing atom modelled with a core-hole. A cubic spline procedure was used to smooth the data on the supported sample (C), with careful inspection to check that this did not distort the spectrum. All data were analysed with the EXAFS bearing the same *k*-space weighting, *viz.* $k^2 \cdot \chi(k)$ [*k* is the wave vector (\AA^{-1}), $\chi(k)$ is the normalised EXAFS amplitude]. The shell occupation numbers were fixed for the values expected for the species under study. The parameters AFAC (proportion of absorption causing EXAFS) and VPI (due to inelastic scattering of the photoelectron)¹⁷ were maintained at 0.9 and -4 eV respectively. Fourier transforms were corrected for the phase shifts of the carbon shell.

Results

$[\text{Os}_3(\text{CO})_{12}]$ (1) on Silica.— $[\text{Os}_3(\text{CO})_{12}]$ solutions were heated to reflux with Aerosil 200 under an atmosphere of N_2 in cyclohexane, n-octane, and nonane. No reaction was observed in cyclohexane. Reaction in n-octane gave a bright yellow oxide at 5 h showing an i.r. spectrum with $\nu(\text{CO})$ absorptions at 2 114w, 2 077s, 2 067s, 2 024s, 2 015 (sh), and 1 984m cm^{-1} , and labelled species (A). Comparison with previous work indicates this is $[\text{Os}_3\text{H}(\text{CO})_{10}(\mu\text{-O-oxide})]$ (2).⁴ Reaction in nonane for 15 h afforded a material giving a similar i.r. spectrum, but the band at 2 114 cm^{-1} was obscured by a stronger, broader feature at 2 121 cm^{-1} . After 2 d, in nonane the material showed three broad absorptions at 2 125w, 2 036s, and 1 953 cm^{-1} , although bands due to species (A) could still be detected.

Vacuum pyrolysis at 160 °C of species (A) caused a gradual

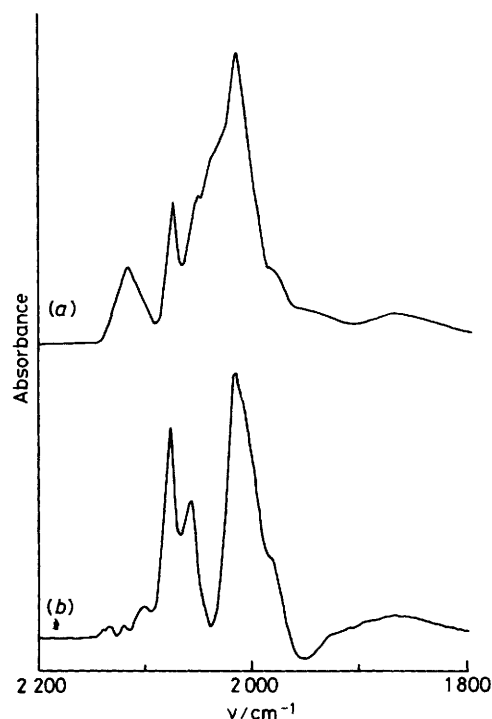


Figure 1. (a) I.r. spectrum of (B) + CO (300 Torr) + H_2O (20 Torr) after 24 h at 290 °C. (b) I.r. difference spectrum with the spectrum of (B) subtracted out

change towards an off-white material showing three broad i.r. bands at 2 126m, 2 036s, and 1 952m cm^{-1} after 19 h, called species (B). This, in turn, was heated in a sealed vessel with CO (440 Torr, 235 °C) for 66 h, and the resulting material showed a loss in intensity of the band at 1 952 cm^{-1} and a feature at $\sim 2 080$ cm^{-1} . A clearer spectrum was obtained by the addition of water to this system [CO (300 Torr) + H_2O (20 Torr) at 290 °C for 24 h]. The i.r. spectrum of this material is shown in Figure 1(a). A difference spectrum subtracting out bands due to residual (B), Figure 1(b), contains i.r. absorptions clearly attributable to species (A), demonstrating the partial reverse of the transformation *in vacuo*, assisted by the presence of water vapour.

The pyrolysis of (A) to (B) was monitored on a pressed disc of (A), at 140 °C, a method which has been shown to cause high-frequency shifts to $\nu(\text{CO})$ bands compared to Nujol mull.^{1,2} Loss of (A) was complete after 40 min. Further heating for a period of 15 h caused the disc to acquire dark spots, suggesting gross metal aggregation subsequent to the formation of (B). Throughout this period the relative intensities of the three bands remained constant. Exposure of this disc to CO (300 Torr) at 80 °C caused a slow increase in intensity of the two higher frequency bands (2 126 and 2 043 cm^{-1}), whilst the third absorption (1 973 cm^{-1}) remained unchanged. This implies two components, (B1) and (B2).

Diffuse-reflectance electronic spectra were obtained for (A) and (B), and are compared with some osmium cluster complexes in Table 1. As has been reported previously,⁹ absorptions are observed near 400 nm, consistent with the presence of metal-metal bonding. The electronic spectrum of (A) is compared with that of $[\text{Os}_3\text{H}(\text{CO})_{10}(\mu\text{-OPh})]$ in cyclohexane solution in Figure 2, and appears to provide evidence for the formulation of (A) as species (2). The agreement with the spectrum of $[\text{Os}_3(\text{CO})_{10}(\mu\text{-OMe})_2]$ is much poorer. More disturbingly, agreement with $[\text{Os}_3\text{H}(\text{CO})_{10}(\mu\text{-OPh})]$ is also poor, so the match shown in Figure 2 may be fortuitous.

Table 1. Electronic spectroscopic data for dissolved and supported osmium complexes

Complex	$\lambda_{\text{max.}}/\text{nm}$ ($10^{-4} \epsilon/\text{dm}^3 \text{ mol}^{-1} \text{ cm}^{-1}$)
(1) $[\text{Os}_3(\text{CO})_{12}]^a$	386 (0.38), 334 (1.05), 248 (2.76), 215 (2.52)
$[\text{Os}_3\text{H}_2(\text{CO})_{10}]^a$	581 (0.02), 333 (0.54), 292 (0.43), 240 (0.77), 215 (0.89)
$[\text{Os}_3\text{H}(\text{CO})_{10}(\mu\text{-SP}^n)]^a$	392 (0.27), 326 (0.56), 253 (1.09), 219 (1.72)
$[\text{Os}_3\text{H}(\text{CO})_{10}(\mu\text{-OPh})]^a$	400w, 350w (sh), 308m, 219s (sh)
$[\text{Os}_3\text{H}(\text{CO})_{10}(\mu\text{-OMe})]^a$	310w (sh), 286w (sh), 262m, 238s, 214s
$[\text{Os}_3(\text{CO})_{10}(\mu\text{-OMe})_2]^a$	332mw, 296m, 267m, 203s
$[\text{Os}_3\text{H}_2(\text{CO})_9(\mu_3, \eta\text{-C}=\text{CH}_2)]^a$	425w, 351m, 276s, 228s
$[\text{Os}_4\text{H}_4(\text{CO})_{12}]^b$	319 (0.16), 239 (0.27), 222s
$[\text{Os}_6(\text{CO})_{18}]^a$	442w, 348m, 251m, 203s
(A) (yellow) ^c	402m, 353m, 303s, 252s
(B) (off-white) ^c	394w, 321m, 232s
(C) (yellow) ^d	374s, 335s, 301s, 248s
(D) (off-white) ^d	415vw, ~380w (sh), 309m, 225s

^a In cyclohexane. ^b In CH_2Cl_2 . ^c On SiO_2 . ^d On Al_2O_3 .

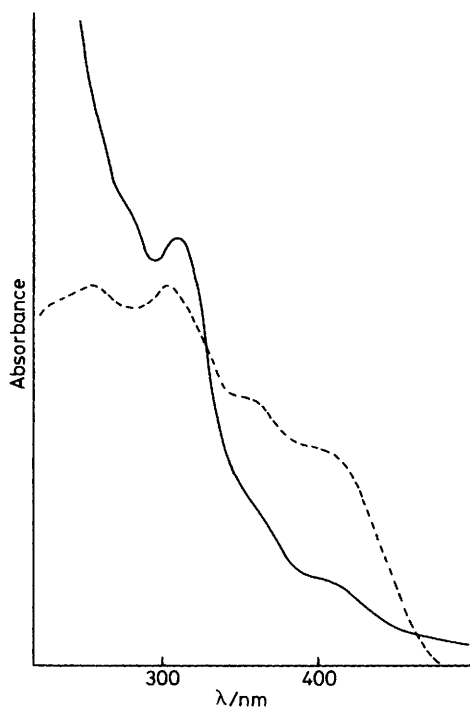


Figure 2. Diffuse-reflectance electronic spectrum of (A) (on silica) (---) compared with the absorption spectrum of $[\text{Os}_3\text{H}(\text{CO})_{10}(\mu\text{-OPh})]$ in cyclohexane solution (—)

The results obtained here are consistent with previous proposals that the two components of (B) differ in their Os:CO ratio.^{4,9} One species, (B1), contains absorptions at the higher two frequencies (2126 and 2036 cm^{-1}). A ^{13}C O-enriched sample of (B) was synthesised and exhibited bands at 2107m, 2030s, 2002 (sh), and 1929w cm^{-1} (Figure 3) in a Nujol mull. This immediately discounts any possibility that any surface species (B) is a monocarbonyl. For example, if the highest frequency band was due to a monocarbonyl, a band with the full isotope shift from 2120 cm^{-1} would expect to give rise to a ^{13}C O band at 2073 cm^{-1} , which was not observed. The isotopic

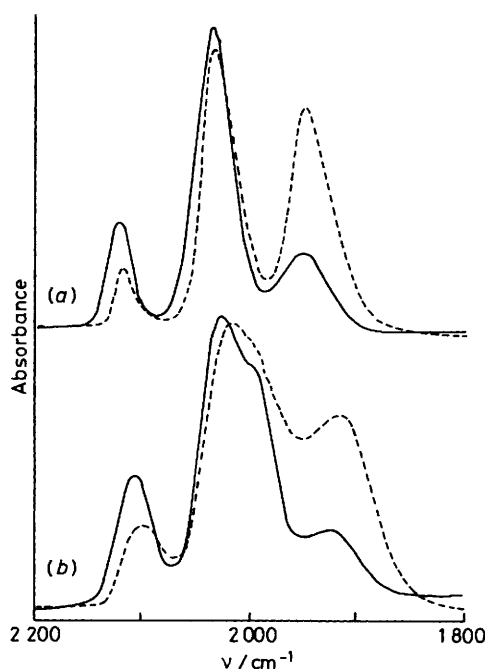


Figure 3. I.r. spectra of (B) (—) on silica and (D) (---) on alumina: (a) natural abundance CO, (b) ^{13}C O enriched

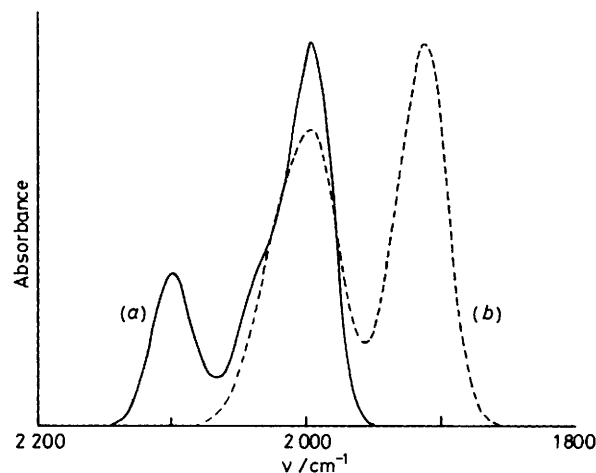


Figure 4. Computed i.r. spectra of the $\nu(\text{CO})$ bands of the silica supported species (B): (a) (B1) using a $[\text{Os}(\text{CO})_3]_2$ model with 80% ^{13}C O, (b) (B2) using a $[\text{Os}(\text{CO})_2]_3$ model with 80% ^{13}C O

shift for the high frequency band was calculated for a range of mononuclear models which would give two $\nu(\text{CO})$ bands as seen for (B1) for the ^{13}C O-enrichment range of 50–90%. {The ^{13}C O content of the $[\text{Os}_3(\text{CO})_{12}]$ used was estimated as 70–80%.} The models tested were $\text{C}_{2v} \text{M}(\text{CO})_2$, $\text{C}_{3v} \text{M}(\text{CO})_3$, and $\text{C}_{4v} \text{M}(\text{CO})_4$. At an enrichment level of 75%, none of these models produced agreement with the position of the band at 2107 cm^{-1} that was closer than 2097 cm^{-1} , suggesting that (B1) contains more than four carbonyl groups. Two models (i) and (ii), of greater complexity (data in Table 2), were then employed.

(i) Cyclic $[\text{Os}(\text{CO})_2]_3$. For model (i), the high frequency band consisted of 44 components and when plotted for a 70% ^{13}C O content using a 25- cm^{-1} linewidth yielded a band at 2097 cm^{-1} with a shoulder at 2069 cm^{-1} , which is not in accord with the experimental spectrum. Also the intensity gain in the disc

Table 2. Parameters used for the models in the mixed-isotope intensity calculations

System modelled	Structure	Force constants (mdyn Å ⁻¹)	Angles (°)	¹³ CO level (%)
(B1)		K 17.37 k_{12} 0.6 $k_{23} = k_{24} = k_{25} = k_{16} = 0.05$	θ_{12} 123 θ_{13} 99 θ_{14} 52	70
(B1)		K 17.20 k_{12} 0.41 k_{16} 0.05 k_{14} 0.08 k_{25} 0.02 k_{15} 0.03	θ_{12} 99 θ_{14} 123 θ_{15} 52	0, 70, 80
(B2)		K 16.03 k_{12} 0.6 $k_{23} = k_{24} = k_{25} = k_{16} = 0.05$	θ_{12} 90 θ_{13} 75.5 θ_{14} 41.4	70, 80
(B2)		K 16.1 k_{12} 0.75 k_{13} 0.078 k_{14} 0.057	θ_{12} 90 θ_{13} 120 θ_{14} 60	70, 80

pyrolysis experiments of the natural abundance CO sample of (B) under CO indicated relative intensities of 1:~3.4 for the 2 126 and 2 043 cm⁻¹ bands of (B1). This would fit an OC-M-CO angle of ~123°, larger than observed in free carbonyls and so this model was discounted.

(ii) [Os(CO)₃]₂. Spectra were calculated for an eclipsed geometry with local C_{3v} symmetry at each metal centre, the C₃ axes being perpendicular to the M-M bond. The calculated spectra are presented in Figure 4(a) for 80% ¹³CO. Although agreement has improved, there is still a 6-cm⁻¹ error in the position of the high frequency band of the enriched sample. In addition, while the major feature in the calculated spectrum matches the experimental feature at 2 000 cm⁻¹, the feature at 2 030 cm⁻¹ is not reproduced. A OC-M-CO bond angle of 99° would be required to give the observed intensity ratio for (B1); angles greater than this are apparent in [Os₃H₂(CO)₉S] and so this value seems feasible.¹⁹ This compares with the value of 92° in a previous report for a mononuclear model.¹¹

The i.r. band assigned to species (B2) is observed at 1 954 cm⁻¹ for the ¹²CO sample and at ~1 929 cm⁻¹ for the isotopically enriched sample, a shift inconsistent with a mononuclear monocarbonyl. A second i.r. feature due to (B2) appears to be coincident with the lower frequency band of (B1). Although an accurate determination of the relative intensities of the bands due to (B2) was not possible, these appeared to be comparable and a value of 1:1 was used for subsequent calculations. The isotopic shift for the low-frequency band of this pair was calculated, assuming ¹²CO frequencies of 2 040 and 1 954 cm⁻¹, for C_{2v} M(CO)₂, C_{3v} M(CO)₃, C_{4v} M(CO)₄, and C_{2v} [M(CO)₂]₂. All of these models overestimate the shift of the low-frequency band by 10–15 cm⁻¹. Spectra were also calculated for a cyclic [M(CO)₂]₃ model, and gave rise to calculated band positions of 1 919 and 1 916 cm⁻¹ for 70 and 80% ¹³CO levels [Figure 4(b)].

[Os₃(CO)₁₂] (I) on Alumina.—No reaction was observed when a suspension of alumina was refluxed in a solution of [Os₃(CO)₁₂] in cyclohexane. However, after refluxing in n-heptane for 6 h, a yellow solid was obtained which exhibited ν(CO) i.r. absorptions at 2 105w, 2 063m, 2 050m, 2 017s, and 1 987 (sh) cm⁻¹, labelled species (C). Reaction in n-octane for 2 h afforded a similar material but extending the reflux time to 17 h

produced an off-white oxide with three broad ν(CO) bands at 2 120m, 2 027s, and 1 947s cm⁻¹, species (D). I.r. spectra of the reaction solutions showed the presence of a new complex, identified as [Os₃H(Cl)(CO)₁₀] on the basis of its published i.r. spectrum,²⁰ and by matching an experimentally determined mass spectral isotope pattern with calculated values.

Disc pyrolysis experiments were carried out to monitor the decomposition of species (C). Vacuum pyrolysis at 110 °C caused conversion to (D) after 2.5 h (2 119w, 2 028s, and 1 943 cm⁻¹). Addition of CO (300 Torr) at 90 °C for 5 h caused a lowering of the relative intensity of the lowest frequency band (2 120w, 2 034s, and 1 954w cm⁻¹). Little change was observed after a further 16 h. Experiments with powdered samples confirmed the parallel with the behaviour on silica and that (D) itself was also two coexisting species (D1) [ν(CO) 2 120 and ~2 027 cm⁻¹] and (D2) [ν(CO) ~2 027 and 1 947 cm⁻¹]. No evidence for the conversion of (D) back to (C) was obtained.

Diffuse-reflectance electronic spectra were recorded for (C) and (D). These again exhibited bands near 400 nm, which may be due to transitions within the metal-metal molecular orbital manifold. The spectra differ from those of species (A) and (B) on silica. The spectrum of (C) is similar to that reported by Deeba *et al.*⁶

Mixed-isotope experiments were carried out on a ¹³CO-enriched sample of (D). The i.r. spectra of natural abundance and ¹³CO-enriched versions are presented in Figure 3 and compared with the silica counterparts. Features of the enriched sample were observed at 2 101w, 2 009s, and 1 917 cm⁻¹. Compared to the silica spectra, the proportion of the species with the lower frequency bands has increased. The observed frequency shifts on enrichment were similar on the two supports, confirming the analogous nature of (B) and (D).

EXAFS Studies of the [Os₃(CO)₁₂]-Alumina Products.—Model compounds. The primary objective of the Os L(III) edge EXAFS experiments was the determination of the structure of the surface species on alumina, (C). Three model complexes were investigated, *viz.* [Os₃(μ-H)₂(CO)₁₀] (4), [Os₃(μ-H)(CO)₁₀(μ-OMe)] (5), and [Os₃(CO)₁₀(μ-OEt)₂] (6). These were used to ascertain whether the structural details of the isoscelean metal triangles in (4) and (6), and the bridging oxygen atoms in (5) and (6) could be observed by EXAFS. The data on

Table 3. EXAFS spectroscopically derived distances (\AA) and Debye-Waller factors ($\alpha = 2\sigma^2$)^a (\AA^2) for model compounds, with X-ray diffraction distances in parentheses

Compound	Fit index	E_0 ^b /eV	Os-C	α	Os...O ^c	α	Os-O	α	Os-Os ^d	α	Os-Os ^e	α
(4)	0.111	16.2	1.93	0.008	2.91	0.015			2.83	0.010	2.64	0.013
			(1.92)		(3.05)				(2.82)		(2.68)	
(5)	0.113	16.8	1.91	0.008	2.91	0.018	2.24	0.016	2.81	0.012	2.81	0.012
			(1.91)		(3.05)		(2.10)		(2.82)		(2.82)	
(6)	0.060	18.6	1.90	0.010	2.90	0.016	2.24	0.019	2.82	0.016	3.08	0.011
			(1.87)		(3.04)		(2.09)		(2.82)		(3.08)	

^a σ^2 = Mean square variation in bond length. ^b E_0 = Energy origin of the photoelectron. ^c Carbonyl oxygen. ^d Non-bridged Os-Os. ^e Bridged Os-Os.

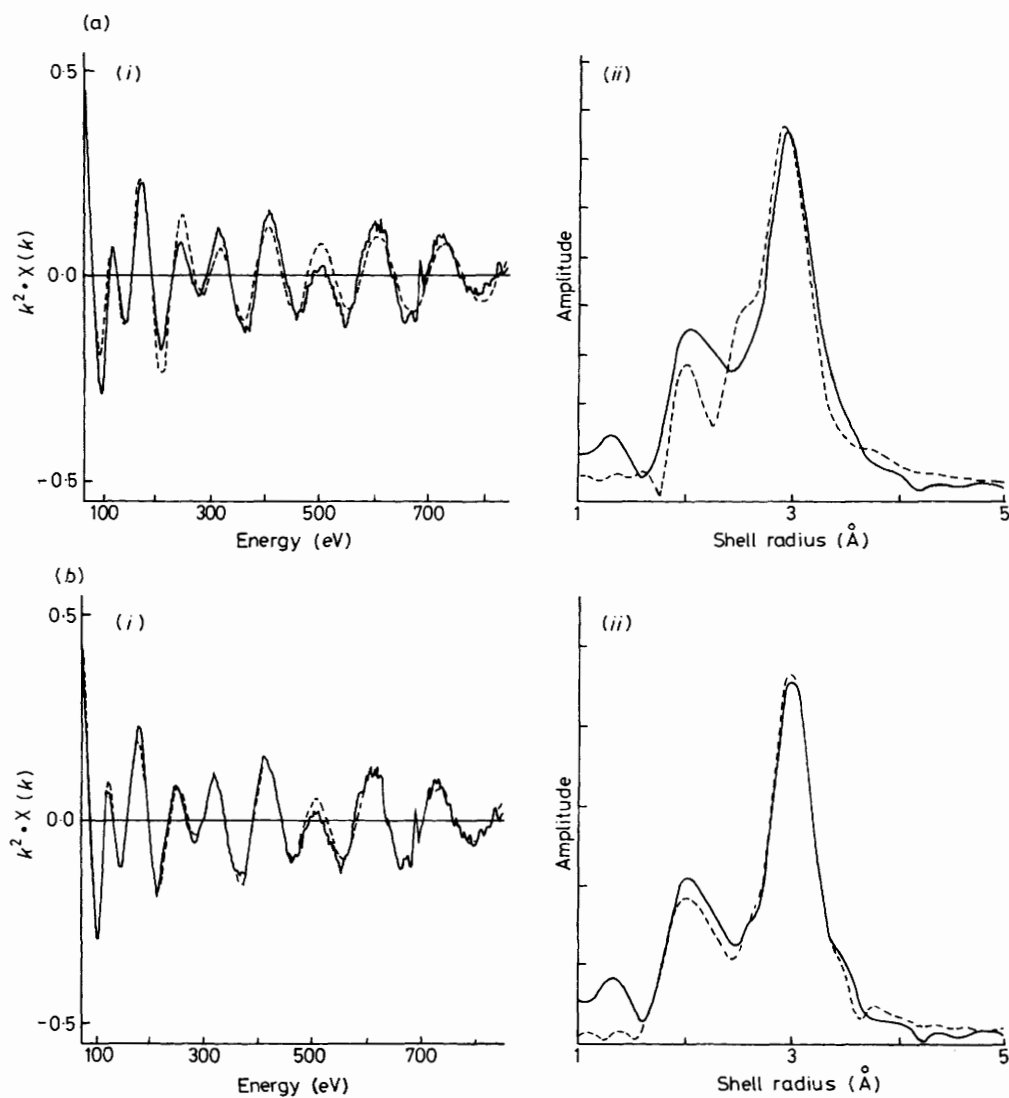


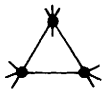
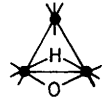
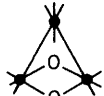
Figure 5. Os L(III) edge EXAFS (i) and Fourier transforms (ii) of $[\text{Os}_3(\text{CO})_{10}(\mu\text{-OEt})_2]$ (6). Experimental (—) and calculated (---) plots for (a) a three-shell model [Os-C = 1.92 \AA , α = 0.013 \AA^2 ; Os-Os = 2.82 \AA , α = 0.010 \AA^2 ; Os...O(carbonyl) = 2.91 \AA , α = 0.020 \AA^2 ; E_0 = 18.3 eV; fit index = 0.161] and (b) a five-shell model (details as in Table 3)

these complexes were modelled with structures of increasing complexity. In Figure 5 we present a comparison between the fits for $[\text{Os}_3(\text{CO})_{10}(\mu\text{-OEt})_2]$ with a three-shell model (one Os-Os distance plus the carbonyl groups) and a five-shell model, reflecting the geometry in $[\text{Os}_3(\text{CO})_{10}(\mu\text{-OMe})_2]$ ²¹ [shells due to Os-C, Os-O, Os-Os, Os...O (carbonyl), and

Os...Os]. Inclusion of the extra shells clearly gives a better match of the EXAFS data, with a lower fit index, and also of the Fourier transform.

Details of the parameters obtained for these model compounds are presented in Table 3. Generally good estimates of Os-C and Os-Os distances were obtained. The Os-O bond

Table 4. Analysis of the Os *L*(III) EXAFS data of species (C) on alumina for three models

Model	Fit index	E_0 /eV	Os-C	α	Os...O ^a	α	Os-O	α	Os-Os ^b	α	Os-Os ^c	α
 [Os ₃ (CO) ₁₀]	0.292	18.1	1.93	0.024	2.90	0.026			2.84	0.009		
 [Os ₃ H(CO) ₁₀ (μ -O)]	0.187	19.7	1.91	0.016	2.90	0.026	2.25	0.005	2.84	0.009	2.84	0.009
 [Os ₃ (CO) ₁₀ (μ -O) ₂]	0.185	20.2	1.90	0.012	2.89	0.018	2.24	0.016	2.84	0.006	3.13	0.010

^a Carbonyl oxygen. ^b Non-bridged Os-Os. ^c Bridged Os-Os.

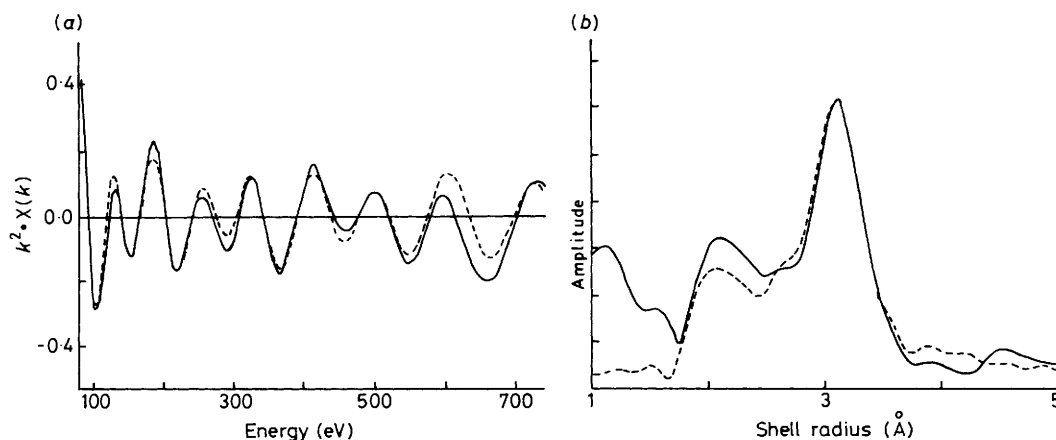


Figure 6. Os *L*(III) edge EXAFS (a) and Fourier transforms (b) of species (C) on alumina. Cubic splined experimental data (—) and calculated (---) plots for a model with structure (3)

distances were consistently overestimated by 0.14 Å, while the Os to carbonyl oxygen separations were consistently underestimated by a similar value. This indicates a deficiency in the oxygen phase shifts employed and probably also strong double and triple scattering effects within the linear M-C-O unit. These effects will be the subject of a future report, but the consistency of these discrepancies would indicate that they were transferable to the surface species (C).

Some non-crystallographic models were also investigated to test the methodology required for analysing data on the supported system. Introduction of dummy Os-O shells in [Os₃(CO)₁₂] caused only slight changes in the fit index, but yielded unrealistic α values of 0.03–0.05 Å². Attempting to fit the EXAFS of [Os₃(CO)₁₀(μ -OEt)₂] with a single-bridging oxygen site afforded α values of \sim 0.008 Å². A bridging oxygen site bears the fingerprint of an apparent shell radius of \sim 2.24 Å and an α value of \sim 0.018 Å².

Obtaining *a priori* evidence for the isoscelean triangles was found to be very difficult. Artificially adding a second Os-Os shell in the analysis of [Os₃(CO)₁₂] and [Os₃(μ -H)(CO)₁₀(μ -OMe)] gave a refined distance of \sim 3.1 Å. There was no

consistent trend in either the fit index or the Debye-Waller factors. So the evidence for distortions of *ca.* 0.2 Å from an equilateral metal triangle from EXAFS data in carbonyl complexes is inconclusive.

Alumina supported systems. Since the i.r. evidence for the Os₃(CO)₁₀ group in species (C) was strong, three models were used to analyse the EXAFS data for the alumina supported cluster. These were a three-shell model [Os-C, Os-Os, and Os...O(carbonyl)], structure (2), analogous to [Os₃(μ -H)(CO)₁₀(μ -OMe)], and structure (3), analogous to [Os₃(CO)₁₀(μ -OEt)₂]. The results of these analyses are presented in Table 4, and the fit of the EXAFS and Fourier transform for structure (3) is shown in Figure 6. Inclusion of the bridging oxygen site causes a substantial improvement in the fit of both EXAFS and Fourier transform and is evidently necessary. As to be expected from the analyses on the model compounds, distinguishing between structures (2) and (3) is not straightforward. These models give similar fit indexes as well as the expected shell radii and plausible values for the Os₃(CO)₁₀ moiety. The bridging oxygen is also located at the expected apparent distance. Only the Debye-Waller factor for this shell offers any discrimination.

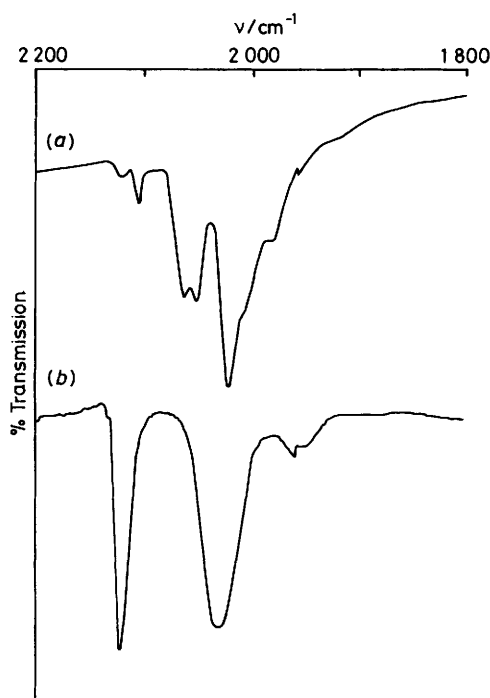


Figure 7. I.r. spectra of $[\text{Os}_3(\text{CO})_{12}]$ on titania: (a) after reaction in refluxing *n*-heptane for 5 h, (b) the sample after pyrolysis *in vacuo* (160°C , 15 h)

The value of 0.016 \AA^2 observed for structure (3) is clearly in the range observed for the model compounds. It seems unlikely that the combination of static disorder and mean correlated vibrational motion of the Os–O unit will be markedly reduced on changing from a crystalline environment to the surface of an amorphous oxide. So we tentatively suggest that the EXAFS evidence on this sample of species (C) favours a bis-oxygen bridged species of the type (3).

A sample of (D) was studied by EXAFS of the Os *L*(III) edge in transmission mode. However the data quality was insufficiently good for other than the estimation of the number of carbonyl groups at between two and three per osmium atom. The signal-to-noise level over 500 eV above the edge position was poor. In this region backscattering from osmium would dominate, whilst the lighter atoms are most important at low *k*. Hence the position of any neighbouring osmium shells could not be determined.

$[\text{Os}_3(\text{CO})_{12}]$ (1) on Titania.—Interaction of titania with a solution of $[\text{Os}_3(\text{CO})_{12}]$ in refluxing heptane for 5 h gave a cream coloured species which exhibited the i.r. spectrum shown in Figure 7(a). After 70 h, only two very weak $\nu(\text{CO})$ bands could be observed at 2119 and $\sim 2025 \text{ cm}^{-1}$. Reaction in refluxing *n*-octane for 22 h gave an off-white material with a three-band $\nu(\text{CO})$ pattern. Pyrolysis of the product from heptane (5 h) at 160°C *in vacuo* for 15 h afforded a very pale grey powder which showed i.r. absorptions at 2120s, 2030s, and $1956\text{w} \text{ cm}^{-1}$ [Figure 7(b)]. The reaction solution after extended reaction times again showed the presence of $[\text{Os}_3\text{H}(\text{Cl})(\text{CO})_{10}]$.

These results are qualitatively similar to those on alumina, although the higher frequency pair of bands are favoured in the pyrolysis product.

$[\text{Os}_3(\text{CO})_{12}]$ on Mica.—A sample of a hydroxylated muscovite mica was interacted with $[\text{Os}_3(\text{CO})_{12}]$ in refluxing *n*-octane for 15 h. The $\nu(\text{CO})$ i.r. bands on the wafer of the mica

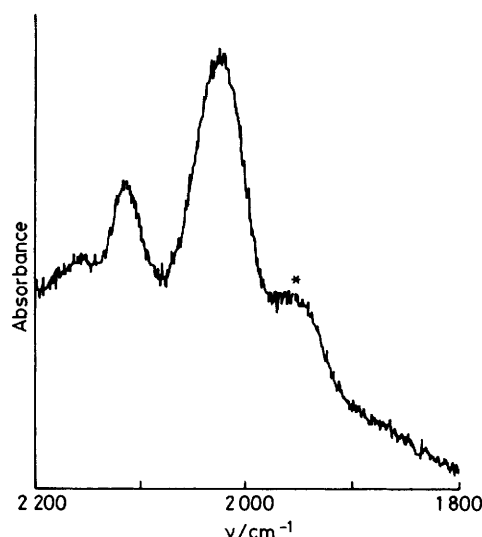


Figure 8. I.r. spectrum of the $[\text{Os}_3(\text{CO})_{12}]$ -mica reaction product measured by ATR. An asterisk indicates the spectrometer grating change

single crystal were recorded by ATR in *ca.* 16 h, Figure 8. Two distinct absorptions were observed at 2117vw and $2020\text{vw} \text{ cm}^{-1}$, together with a probable absorption at 1953 cm^{-1} . This pattern is similar to that of the pyrolysed samples on the three powdered oxide supports. Attempts to determine the surface orientation of these species by polarisation studies were not successful. However, this may well result from the fact that the cleavage plane of muscovite mica contains hydroxyl groups with two different orientations.²²

Discussion

These results confirm observations that the initial chemisorption of $[\text{Os}_3(\text{CO})_{12}]$ (1) on SiO_2 , Al_2O_3 , or TiO_2 gives rise to a species of the form $[\text{Os}_3\text{H}(\text{CO})_{10}(\mu\text{-O-oxide})]$ (2) or $[\text{Os}_3(\text{CO})_{10}(\mu\text{-O-oxide})_2]$ (3).^{4,5} The diffuse-reflectance measurements of the electronic spectrum of species (A) on silica gives supporting evidence to the original formulation of Basset and co-workers³ as the hydride (2). However, the absorption spectrum of the alumina counterpart (C) does not match closely with any of the model compounds, and does not discriminate between (2) and (3). The frequencies of the $\nu(\text{CO})$ absorptions of (C) are of the order of 10 cm^{-1} lower than those of (A). This can occur for two reasons. First, replacement of the hydride ligand by an O–M unit may cause this lowering, as is observed between $[\text{Os}_3\text{H}(\text{CO})_{10}(\text{OPh})]$ and $[\text{Os}_3(\text{CO})_{10}(\text{OPh})_2]$ (difference *ca.* $5\text{--}7 \text{ cm}^{-1}$).⁴ Secondly, alumina appears to behave as a less electron-withdrawing ligand than silica, and can also cause a frequency change in the same direction. EXAFS analyses of the model compounds demonstrated that the isoscelean metal triangle anticipated for structure (3) could not be detected reliably. Only the Debye–Waller factor for the Os–O shell gives any evidence in favour of the presence of (3) on alumina. The surface of γ -alumina is considered to be mainly the (100) plane of a defect spinel lattice,²³ with drying at $\sim 100^\circ\text{C}$ maintaining a fully hydroxylated surface. By using the crystallographic geometries for models of (2) and (3),^{21,24} molecular drawings of both models on this surface cause gross interactions between some carbonyl groups and the surface. This can be alleviated for species (2) by considering a special site, either at a step or corner, or by being bound to an aluminium atom [as $\text{Al}(\text{OH})_2$] in a tetrahedral site. For structure (3), even this last option causes substantial steric

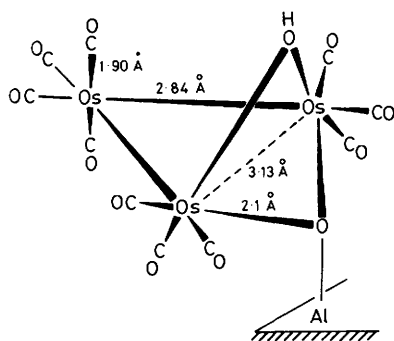


Figure 9. Proposed structure of the species (C) on alumina

interactions which would require rotations of the $\text{Os}(\text{CO})_3$ groups by $\sim 22^\circ$. It seems more probable that the bis-oxygen species (3) should be formulated as $[\text{Os}_3(\text{CO})_{10}(\mu\text{-OAl}\leftarrow)(\mu\text{-OH})]$ as is formed by interaction with adsorbed water. The favoured structure for species (C) is presented in Figure 9, allowing for the 0.14-Å discrepancies in Os-O distances for the model compounds (5) and (6). The initial spectrum obtained on titania contained bands of very similar frequency and relative intensity to those observed on alumina, indicating a similar species on that support also.

Another aim of this work was to ascertain whether the pyrolysis products on these oxides, each of which appears to contain a component of stoichiometry $\text{Os}(\text{CO})_3$ [(B1) and (D1)] and another of stoichiometry $\text{Os}(\text{CO})_2$ [(B2) and (D2)], contained monomeric units or aggregates. However the broadness of their bands rendered this extremely difficult. Nevertheless, the use of the mixed-isotope experiments did add support to these stoichiometries. First, there was a clear absence of any bands with a full $^{12}\text{CO}/^{13}\text{CO}$ isotopic shift, indicating that none of the major species giving rise to the $\nu(\text{CO})$ i.r. bands was a monocarbonyl. Secondly, the computer simulations of the bands assigned to (B1) discounted this being an $\text{Os}(\text{CO})_2$ group, both because of the large OC-Os-CO angle required (123°), and also the overestimation of the band shifts in the ^{13}CO -enriched spectrum. However, none of the models tried gave a satisfactory fit of the enriched spectrum. The cyclic $[\text{M}(\text{CO})_2]_3$ and $[\text{M}(\text{CO})_3]_2$ models provided the closest fit of the lower frequency bands due to (B2). This suggests a cyclic $[\text{M}(\text{CO})_3]_3$ analogue as a more satisfactory model of (B1). Simulating this model would require many structural and vibrational assumptions and thus was not attempted. Larger metal aggregates present even greater difficulties. These suggestions, however, of close arrays of trimers would readily account for the regeneration of species (2) from the material (B). It is also consistent with the proposals based on electron microscopic results.¹³ Additional evidence comes from an EXAFS study of the pyrolysis product of $[\text{Os}_3\text{H}_2(\text{CO})_{10}\{\text{Ph}_2\text{-P}(\text{CH}_2)_3\text{Si}(\text{OEt})_{3-x}(\text{O-oxide})_x\}]$, where oxide = silica,²⁵ which displays a similar i.r. spectrum to that of (B).²⁶ Backscattering from approximately two Os neighbours was detected, albeit at bonding distances. This, in turn, would be consistent with the electronic spectroscopic data of (B) and (D).

Two further points are of note. First, the initially observed product on the mica single crystal surface is very similar in form to the pyrolysis products on the three oxide samples, with the analogue of (B1) predominating over (B2). The stability of the initial species (2) or (3) on various surfaces is in the order silica > alumina > titania \gg mica. Secondly, the detection of $[\text{Os}_3\text{H}(\text{Cl})(\text{CO})_{10}]$ in solution indicates that adventitious chlorine on the surface of alumina and titania can be scavenged by the osmium clusters and possibly affect the course of the surface reaction.

Considerable variations in behaviour are noted between rhodium, ruthenium, and osmium carbonyls on oxide supports. For rhodium, oxidation has been shown to cause fragmentation to isolated $\text{Rh}^1(\text{CO})_2$ and (on titania) $\text{Rh}^1(\text{CO})_{2-3}$ sites, in addition to the conversion of $[\text{Rh}_4(\text{CO})_{12}]$ into $[\text{Rh}_6(\text{CO})_{10}]$ during the initial chemisorption. The chemistry of $[\text{Ru}_3(\text{CO})_{12}]$ on oxide surfaces is highly complex. Only on silica was an analogue to (2) observed,^{2,27} viz. $[\text{Ru}_3\text{H}(\text{CO})_{10}(\mu\text{-O-oxide})]$. The evidence from i.r. and u.v.-visible studies indicated that no sites had more than two CO groups per ruthenium and also the formation of oligomers of the form $[\text{Ru}(\text{CO})_2]_n$ ($n = 2$ or 3). Subsequent reactions generated a variety of di- and monocarbonyl sites in varying oxidation states. In the case of osmium, the initial chemisorption complex, (2) or (3), is substantially more stable and can be observed on silica, alumina, and titania. The subsequent reactions then appear less diverse than for ruthenium, at least for the major carbonyl bearing species; there is e.s.r. evidence for minor odd-electron species also. All evidence appears to indicate the coexistence of $[\text{Os}(\text{CO})_3]_n$ and $[\text{Os}(\text{CO})_2]_n$ species. The present work suggests that n is greater than 2.

Acknowledgements

We wish to thank the S.E.R.C. for research studentships (to S. L. C. and G. S. McN.), Degussa Ltd. for the oxide samples, and Johnson Matthey for the loan of osmium tetroxide.

References

- J. Evans and G. S. McNulty, *J. Chem. Soc., Dalton Trans.*, 1984, 587.
- J. Evans and G. S. McNulty, *J. Chem. Soc., Dalton Trans.*, 1984, 1123.
- B. Besson, B. Morawek, A. K. Smith, J. M. Basset, R. Psaro, A. Fusi, and R. Ugo, *J. Chem. Soc., Chem. Commun.*, 1980, 569.
- R. Psaro, R. Ugo, G. M. Zanderighi, B. Besson, A. K. Smith, and J. M. Basset, *J. Organomet. Chem.*, 1981, **213**, 215.
- M. Deeba and B. C. Gates, *J. Catal.*, 1981, **67**, 303.
- M. Deeba, B. J. Steusand, G. L. Schrader, and B. C. Gates, *J. Catal.*, 1981, **69**, 218.
- M. Deeba, J. P. Scott, R. Barth, and B. C. Gates, *J. Catal.*, 1981, **71**, 373.
- S. L. Cook, J. Evans, and G. N. Greaves, *J. Chem. Soc., Chem. Commun.*, 1983, 1287.
- G. Collier, D. J. Hunt, S. D. Jackson, R. B. Moyes, I. A. Pickering, P. B. Wells, A. F. Simpson, and R. Whyman, *J. Catal.*, 1983, **80**, 154.
- E. O. Ebudunmi, Y. Zhao, H. Knözinger, B. Tesche, W. H. Manogue, B. C. Gates, and J. Hulse, *J. Catal.*, 1984, **86**, 95.
- H. Knözinger and Y. Zhao, *J. Catal.*, 1981, **71**, 337.
- V. A. Shvets, A. L. Tarasov, V. B. Kazansky, and H. Knozinger, *J. Catal.*, 1984, **86**, 223.
- J. Schwank, L. F. Allard, M. Deeba, and B. C. Gates, *J. Catal.*, 1983, **84**, 27.
- B. F. G. Johnson, J. Lewis and P. A. Kilty, *J. Chem. Soc. A.*, 1968, 2859.
- E. Pantos, Daresbury Laboratory Preprint, DL/SCI/P346E, 1982.
- P. A. Lee and J. B. Pendry, *Phys. Rev.*, 1975, **11**, 2795.
- S. J. Gurman, N. Binsted, and I. Ross, *J. Phys. C*, 1984, **17**, 143.
- E. Pantos and G. D. Firth, Daresbury Laboratory Technical Memorandum, DL/CSE/TM21, 1982.
- B. F. G. Johnson, J. Lewis, D. Pippard, P. R. Raithby, G. M. Sheldrick, and K. D. Rouse, *J. Chem. Soc., Dalton Trans.*, 1979, 616.
- A. J. Deeming and S. Hasso, *J. Organomet. Chem.*, 1976, **114**, 313.
- V. F. Allen, R. Mason, and P. B. Hitchcock, *J. Organomet. Chem.*, 1977, **140**, 297.
- J. M. Serratosa and W. F. Bradley, *J. Phys. Chem.*, 1958, **62**, 1164.
- J. B. Peri, *J. Phys. Chem.*, 1965, **69**, 211, 220.
- M. R. Churchill and H. J. Wasserman, *Inorg. Chem.*, 1980, **19**, 2391.
- N. Binsted, S. L. Cook, J. Evans, and G. N. Greaves, *J. Chem. Soc., Chem. Commun.*, 1985, 1103.
- S. C. Brown and J. Evans, in preparation.
- A. Theolier, A. Choplin, L. D'Ornelas, J. M. Basset, G. Zanderighi, R. Ugo, R. Psaro, and C. Sourisseau, *Polyhedron*, 1983, **2**, 119.

Received 21st December 1984; Paper 4/2157